Modelling colossal magnetoresistance manganites

2007 J. Phys.: Condens. Matter 19 125211

(http://iopscience.iop.org/0953-8984/19/12/125211)

IOP PUBLISHING JOURNAL OF PHYSICS: CONDENSED MATTER

J. Phys.: Condens. Matter **19** (2007) 125211 (26pp) doi:10.1088/0953-8984/19/12/125211

Modelling colossal magnetoresistance manganites

T V Ramakrishnan

Department of Physics, Banaras Hindu University, Varanasi-221005, India

E-mail: tvrama@bhu.ac.in

Received 11 September 2006
Published 6 March 2007
Online at stacks.iop.org/JPhysCM/19/125211

Abstract

Rare-earth (Re) manganites (with alkaline-earth (Ak) ions partially substituting them), i.e. $Re_{1-x}Ak_xMnO_3$, have been intensively explored for the last decade or more because of the promise of magnetoelectronic applications as well as because of complex and unusual phenomena in which electronic, structural and magnetic effects are intertwined. A brief survey of these and a description of the three strong local interactions of the e_g electrons (in two different orbital states at each site), namely with Jahn–Teller phonon modes (strength g), with resident t_{2g} spins (ferromagnetic Hund's rule coupling J_H) and between each other (the Mott–Hubbard correlation U) form the background against which efforts at modelling manganite behaviour are described. A new two-fluid model of nearly localized (l) polarons and band (b) electrons for low-energy behaviour is hypothesized for large g; some of its applications are mentioned here. First I describe some results of large U, J_H calculations in single-site DMFT (dynamical mean field theory) which includes the effect of all the strong local correlations. These results are directly appropriate for the orbital liquid regime, found typically for $0.2 < x < 0.5$, and not too low temperatures. I show that many characteristic manganite phenomena, such as an insulating ferromagnetic ground state, thermal insulator–metal transition (nearly coincident with the paramagnetic to ferromagnetic transition), colossal magnetoresistance (CMR), materials systematics dependent on the specific Re and Ak ions, and the observed low effective carrier density, can all be understood qualitatively as well as quantitatively. We also discuss the two-'phase' coexistence frequently found in these systems, and show that electrostatic Coulomb interactions mute lb phase separation into nanoscale electronic inhomogeneity with l regions and b puddles. Finally, some problems of current interest as well as general ones arising, e.g. polarons and the physics of large electron phonon coupling g in the adiabatic regime, are mentioned.

(Some figures in this article are in colour only in the electronic version)

1. Introduction

The occurrence of colossal magnetoresistance or CMR in alkaline-earth- (Ak)-doped rare-earth (Re) manganites ($Re_{1-x}Ak_xMnO_3$ with $0 < x < 1$) more than a decade ago [1] has led to widespread exploration of these compounds which were discovered by Jonker and van Santen [2] in the 1950s and studied by them. While the initial impetus was the possibility of magnetic devices based on CMR and related activity continues, it quickly became clear that this family is home to very diverse, unusual and poorly understood phenomena as well as phases. These solid state oxides have emerged as second only to the high-T_c cuprates in the overall global level of research activity; both present fundamental challenges to our understanding of how electrons behave in solids. A number of articles [3–6] and books [7–10] review this field.

1.1. Phenomena

The diversity of phenomena in doped manganites (e.g. [3–10] and references therein) is suggested (figure 1) by the phase diagram of $La_{1-x}Ca_xMnO_3$ [11], a well-studied member of the family. Various kinds of antiferromagnetic insulating phases (e.g. A, Néel, and CE), metallic as well as insulating ferromagnetic states, orbital long order with or without antiferromagnetism, charge order, insulator–metal transitions over a broad range of doping ($0.2 < x < 0.5$), long-range cooperative antiferro-order of Jahn–Teller (JT) distorted octahedra for small x, are all seen to be present. The insulator–metal transition is nearly coincident with the paramagnetic to ferromagnetic or Curie transition (temperature T_c), implying that electronic and magnetic effects are strongly coupled. The connection between structural and electronic properties is illustrated by the fact that while the charge and orbitally ordered structure (with $x \sim 0.5$) forms a superlattice and is electrically an insulator, a relatively small magnetic field destroys this superstructure ('melts' it), and the resulting system is metallic. Other manganites show characteristic similarities and differences. For example, in $La_{1-x}Sr_xMnO_3$, the Curie transition is from a metal to a metal, whereas in $Pr_{1-x}Ca_xMnO_3$ it is best described as insulator to insulator. The transitions between phases are generally of second order. There are however several cases of first-order transition, e.g. the magnetic field induced melting of charge order. Rather than describe further the large number of phenomena in these compounds (references [3–10] give a good idea of these), I mention below three of their striking mutually related general physical characteristics. I do not discuss in detail any specific region (e.g. the fascinating half-doped regime where charge and orbital order are endemic) or a class of effects, but try to focus on common phenomena, basic interactions and models of general significance.

One general characteristic is the persistent proximity of metallic and insulating states. Normally, a system is either a metal or an insulator depending on whether electronic states near the Fermi energy are extended or localized (as they are in Anderson, Mott or band insulators). Consequently, a transition from one to the other occurs only under special conditions of pressure, temperature or composition. However, as can be seen for example from figure 1, $La_{1-x}Ca_xMnO_3$ or LCMO has an insulator to metal transition over the *entire* doping range $0.2 < x < 0.4$ as the temperature is lowered below about 200–300 K. This obviously implies that current carrying extended states and 'insulating' localized states are close to each other in energy over a wide range of doping conditions in this compound, as they are for many others in this family.

Another general characteristic is the extreme sensitivity of physical properties of manganites to small perturbations. Colossal magnetoresistance or CMR (see e.g. figure 2) is perhaps the best known example. Near the Curie transition, the resistivity of most manganites decreases enormously (the fractional change being of order unity) in an external magnetic field

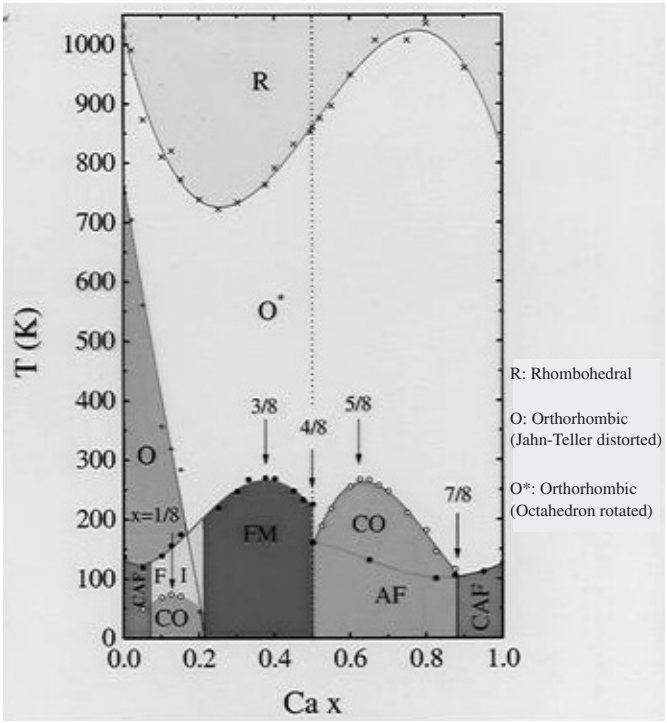

Figure 1. The phase diagram of $La_{1-x}Mn_xO_3$ in the doping x and temperature T plane. The structural phases shown are rhombohedral R, orthorhombic O* with rotated octahedra but without long-range Jahn–Teller (JT) distortion order, and orthorhombic O with rotated octahedra and long-range JT order. CAF (canted antiferromagnetic), FI (ferromagnetic insulator), FM (ferromagnetic metal), CO (charge/orbitally ordered), and AF (Néel antiferromagnetic) regions are also shown. (Adapted from [11]).

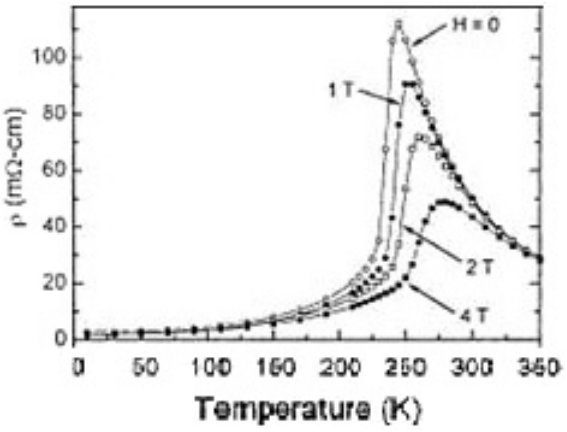

Figure 2. Colossal magnetoresistance as observed in a $La_{0.75}Ca_{0.25}MnO_3$ sample with a Curie temperature T_c of about 230 K. The resistivity is shown as a function of temperature for various values of the field. The change in resistance with magnetic field is seen to be colossal near T_c.

of order a few tesla; the change is two to three orders of magnitude larger than that in a typical metal, where it is generally due to the effect of the magnetic field on the electron trajectory, and is therefore determined by the factor $(\omega_c\tau)^2$, ω_c being the cyclotron frequency and τ the electron relaxation time. The large isotope effect is another instance; the Curie temperature

depends strongly on the oxygen isotopic mass, being for example about 10% higher in LCMO with O^{16} than with O^{18} [12]. Perhaps the ultimate in isotope effects is the observation [13] that the ground state of $(La_{1-y}Pr_y)_{0.7}Ca_{0.3}MnO_3$ for $y = 0.75$ is a metal with O^{16} and an insulator with O^{18}. Finally, the insulating charge/orbitally ordered state (near $x \sim 0.5$) with $T_{CO} \sim 250$ K 'melts' to a metal on application of a magnetic field typically of order 10 T; the Zeeman energy associated with the field is clearly more than an order of magnitude smaller than the charge-ordering energy scale.

Thirdly, there is overwhelming evidence [5, 9] for the simultaneous presence in manganites of two regions or kinds of states on spatial scales varying from nanometres [14] to microns [15] and timescales ranging from less than 10^{-13} s [16–18] to about 10^{-6} s [19] to 10^0 s (static). One of these regions is lattice distorted and insulating while the other has no lattice distortions and is metallic. Often, these regions are referred to as phases, even though they can be nanometres in size and not macroscopic (i.e. not in the thermodynamic limit). Whether such a two-'phase' coexistence is intrinsic to manganites or indeed to all strongly correlated electronic systems (e.g. stripes in cuprates [20] and metal/insulator droplets in a two-dimensional electron gas (2DEG) [21]), being their defining characteristic and related to their 'electronic softness' [22], or whether it is extrinsic is a question of great current interest in the physics of strongly correlated electron systems [22]. I briefly discuss it later in sections 3 and 4.

1.2. Interactions at work

Structurally, the manganites are slightly distorted perovskites ABO_3 which can be viewed as corner-sharing octahedra with the Mn (or B) ions at the centre of the BO_6 octahedron, the O ions at the corners, and the A ions in the interstitial space between octahedra. There is a well-known ideal size for the A ions, and deviation from it in the mean as well as local fluctuations in it due to A-site doping have many interesting and systematic consequences.

I describe now the electronic degrees of freedom relevant for low-energy properties of the manganites, as a preliminary to modelling the low-energy ones. In the MnO_6 octahedron at each lattice site, the s and p orbitals of Mn and O are strongly bonded, so the associated charge transfer levels are well below the Fermi energy. In the octahedral environment of the manganites, the d levels of the Mn ions split into low-lying threefold degenerate t_{2g} states and higher-energy twofold degenerate e_g states separated by about 2 eV, the crystal field energy. In $LaMnO_3$ the four 3d electrons of Mn^{3+} are in a high-spin ($S = 2$) state; the interorbital Coulomb repulsion is large and one is in the weak crystal field regime. The three t_{2g} electrons have a total spin $S = (3/2)$ and are (effectively) ferromagnetically coupled with the e_g electron spin via J_H, the Hund's rule coupling, leading to a total spin $S = 2$. J_H is estimated to be large, about 2–3 eV. On doping with divalent alkaline earths which substitute for the trivalent rare earths, a fraction x of sites has Mn^{4+} ions. At every site then, whether occupied by Mn^{3+} (four 3d electrons, probability $(1 - x)$) or by Mn^{4+} (three 3d electrons, probability x), there are always three t_{2g} electrons, so their only relevant low-energy degree of freedom is spin ($S = (3/2)$), labelled by the spin operator $\mathbf{S}_i$ at site i. The low-energy electronic behaviour is thus determined by the e_g electrons; the ingredients governing their dynamics are mentioned now. An average fraction $(1 - x)$ of the Mn lattice sites is occupied by them in the doped compound, with a fraction x of sites having no e_g electrons.

The two degenerate e_g orbitals ($d_{x^2-y^2}$ and $d_{3z^2-r^2}$) constitute the explicit electronic degrees of freedom at each site. These are often formally described as two components (α, β) of a pseudospin ($S = 1/2$), the corresponding Pauli pseudospin operator being labelled by $\boldsymbol{\tau}$ (with components τ_x, τ_y, τ_z). In a tight-binding d electron model, the nearest-neighbour hopping amplitude for the e_g electron is parameterized by a single number t; the dependence on the orbital states (initial and final) as well as on the spatial direction is determined by the d orbital

wavefunction symmetry, and is given by the matrices $\mathbf{A}_v$ (Slater–Koster factors; see e.g. [23]) below, where v are the Cartesian directions x, y and z.

$$H_{\mathrm{K}} = -(t/4)\sum_{\langle ij\rangle} \mathbf{d}^{+}_{i\sigma}\mathbf{A}_v\mathbf{d}_{j\sigma}. \tag{1}$$

In equation (1), $\mathbf{d}_{j\sigma}$ removes a d electron with spin σ from the site states (α, β) at site j. From the calculated electronic structure [24–30], a bandwidth $2\mathrm{D}_0$ of order 2–4 eV [24–27, 29, 30] is estimated. If parameterized by a tight-binding band, as is done e.g. in [27, 29, 30], the hopping matrix element t is about 0.2–0.3 eV.

Such a model is a simplification and the hopping t represents a second-order term, the primary step being charge transfer from (or to) an oxygen p orbital which is the intermediate state. An explicit dp or two-band model has been discussed in detail (see e.g. [31] for the $LaMnO_3$ end). Here I work with a one- (d-) band model as is common in the field. Some reasons supporting this simplification are the following. First, the 'd' states are local symmetry adapted mixtures of d and p orbitals. Second, the integrated-out 'p' state (or charge transfer band) energy ε_{p} is well away from the Fermi level, so for energies less than $|\varepsilon_{\mathrm{p}} - \varepsilon_{\mathrm{F}}|$, a picture which concentrates on locally d-like states (around each Mn ion site) is accurate. Third, the strong interaction effects of Jahn–Teller coupling as well as J_{H} and U all involve the on-site d state.

As mentioned above, one strong interaction present at each site i is effectively described as ferromagnetic Hund's rule coupling between $\mathrm{t_{2g}}$ spins S_i and $\mathrm{e_g}$ spins s_i, namely

$$H_{\mathrm{Hund}} = \sum_i H^i_{\mathrm{Hund}} = -J_{\mathrm{H}}\sum_i S_i \cdot s_i. \tag{2}$$

It was pointed out very early, by Zener [32] and more pertinently in the way used today by Anderson and Hasegawa [33], that for large J_{H} the effective nearest-neighbour hopping amplitude for $\mathrm{e_g}$ electrons depends on the angle between the corresponding $\mathrm{t_{2g}}$ spins since the $\mathrm{e_g}$ spin direction is enslaved to that of the $\mathrm{t_{2g}}$ spin on the same site, and the $\mathrm{e_g}$ electron conserves its spin direction on intersite hopping. The hopping amplitude and thus the kinetic energy gain due to $\mathrm{e_g}$ electron motion is maximum when the $\mathrm{t_{2g}}$ spins point parallel to each other, i.e. are ferromagnetically aligned. This novel 'double-exchange' ferromagnetic coupling is fundamental to manganites. It implies for example that metallicity (due to $\mathrm{e_g}$ electron motion) and ferromagnetism are strongly connected with each other (see below, section 2, for details and a critique).

It is well known that in the cubic perovskite ABO_3 a quadrupolar ($l = 2$) Jahn–Teller distortion of the BO_6 octahedron removes the twofold degeneracy of the $\mathrm{e_g}$ levels and one of the resulting states is lower in energy. This is prominent in $LaMnO_3$ where below 780 K the distortions order cooperatively ('antiferro' order) while above this temperature there is evidence from EXAFS measurements [34] that it is locally present. The interaction involved can be described as follows. The on-site Jahn–Teller coupling between the $\mathrm{e_g}$ orbitals and lattice modes $\mathbf{Q}_i = Q_{xi}, Q_{zi}$ which are specific combinations of Mn–O bond length changes can be written following Kanamori [35] as $H^i_{\mathrm{JT}} = g\mathbf{d}^{+}_{i\sigma}\boldsymbol{\tau}\mathbf{d}_{is}\cdot\mathbf{Q}_i$, with coupling strength g. The Hamiltonian is, explicitly,

$$H_{\mathrm{JT}} = \sum_i H^i_{\mathrm{JT}} = g\sum_{i,\sigma}(d^{+}_{i\alpha\sigma}\cdot d_{i\alpha\sigma} - d^{+}_{i\beta\sigma}d_{i\beta\sigma})Q_{zi} + g\sum_i (d^{+}_{i\alpha\sigma}d_{i\beta\sigma} + d^{+}_{i\beta\sigma}d_{i\alpha\sigma})Q_{xi}. \tag{3a}$$

The lattice potential energy $V(\mathbf{Q}_i)$ for a displacement $\mathbf{Q}_i$ is given in the harmonic approximation by $(1/2)K\mathbf{Q}_i^2$, where we have assumed the force constants K for the two modes Q_{ix} and Q_{iz} to be the same, which is nearly correct [36]. The lattice or phonon Hamiltonian (for the relevant Einstein-like modes) is

$$H_{\mathrm{ph}} = \sum_i H^i_{\mathrm{ph}} = \sum_i \{V(\mathbf{Q}_i) + (1/2M)p_i^2\}, \tag{3b}$$

where $V(\mathbf{Q}_i) = (1/2)K\mathbf{Q}_i^2$ in the harmonic approximation, and the nearly equal reduced mass M of the modes is approximately that due to oxygen. The two energy eigenvalues of the Jahn–Teller term are $\pm g|\mathbf{Q}_i|$ for an electron present at site i. For the lower-energy state, the total potential energy minimum of $(-g^2/2K) = -E_{\rm JT}$ occurs at $|\mathbf{Q}_i| = Q_0 = (g/K)$ (in the harmonic approximation). $E_{\rm JT}$ is the gain in energy because of Jahn–Teller distortion Q_0. For the other eigenvalue, the potential energy minimum is still at $|\mathbf{Q}_i| = 0$.[1]

The Jahn–Teller mode frequency $\omega_{\rm JT}(=\sqrt{K/M})$ is believed to correspond to an energy of about 0.06 eV, based on the identification of certain Raman spectra peaks with the Jahn–Teller modes [37]. The parameter which describes the strength of the electron lattice coupling is g. It is known to be large in manganites; the related Jahn–Teller energy $E_{\rm JT}$ lies in the range 0.5–2.0 eV [27, 28, 38]. This energy scale is inferred in a number of ways. One is to use the observed Jahn–Teller distortion in $LaMnO_3$, and the measured JT mode frequency $\omega_{\rm JT}$ along with the mode-reduced mass M, and find $E_{\rm JT}$ (or the electron lattice coupling g and the force constant K) using the expressions above [38]. Another is to use results from band structure calculations, e.g. [27], or from cluster calculations. All of these result in an $E_{\rm JT}$ of about 1 eV, the range being from 0.5 to 2 eV.

The electron–phonon coupling g is not expected to change much with doping x, for several reasons. Experimentally, short-timescale experiments [16–18] show that the consequent Jahn–Teller distortion does not change much with x even in $La_{1-x}SrMnO_3$ (LSMO), in the range $0.25 > x > 0.0$. Its reduction by mobile hole screening is expected to be small both because the holes are not very mobile and because the coupling is local; the screening length is a few lattice constants (see e.g. figure 7). The electron–phonon interaction is generally characterized by two dimensionless coupling constants, namely the strength $\lambda\ (=g^2/Kt)$ and the adiabaticity $\gamma\ (=\hbar\omega_{\rm ph}/t)$. In manganites, $\lambda \sim 1$–4, and $\gamma \sim 0.2$–0.3.

The Jahn–Teller distortion Q_0 in $LaMnO_3$ is large, about 0.15 A [39]. This has been known for a long time, and indeed some of the early theories of the 780 K ordering in $LaMnO_3$ modelled it as an order–disorder transition of the local Jahn–Teller distortion already present in each MnO_6 octahedron above the ordering temperature, and supported this hypothesis through the measured integrated entropy change connected with it [40]. The work of Kanamori [35] mentioned above describes the Jahn–Teller and e_g electron degrees of freedom explicitly, and is the basis for studies of the undoped manganite. With the renewed recognition that large Hund's rule coupling effects such as double exchange are prominent in doped manganites, it began to be felt that the Jahn–Teller effect is not essential for phenomena in them. In influential work, Millis, Littlewood and Shraiman [41] and Millis, Muller and Shraiman [42] pointed out that features such as the large resistivity of manganites near the Curie transition (T_c) and the large resistivity change there cannot be understood in terms of only double exchange (or spin) interactions, and that it is essential to include the effect of strong coupling to the lattice leading to polarons.

The third strong on-site interaction is the Mott–Hubbard repulsion. In general, there are several comparable terms here, corresponding to orbital and spin indices of the e_g orbitals, e.g. [43]. Of these, given that for large J_H the e_g electron spin direction is enslaved to that of the t_{2g} spin (so there is no e_g electron spin degree of freedom, effectively) the term of relevance is the repulsion U when the two e_g electrons are in different orbitals. Its actual value is a subject of debate. General trends in perovskite transition metal oxides, photoemission experiments and cluster calculations [24, 43, 44] lead to values ranging from 5 to 10 eV. Distinctly smaller

[1] We note that there is a continuous degeneracy of the local lattice potential $V(\mathbf{Q}_i)$ in the harmonic approximation; it is independent of the direction (given by the angle $\theta_i = \tan^{-1}(Q_{xi}/Q_{zi})$) in which the pseudomagnetic field at site i points, though the eigenstates (the orbital admixtures) depend on it. This is reduced to a discrete threefold degeneracy when cubic anharmonic terms in Q_i are included [35].

values, of order 2–3 eV or so, have been argued for by Millis and others [45]. The value in relation to the bare bandwidth $2D_0$ ($=2zt$ in a nearest-neighbour tight-binding model) of the e_g electrons is obviously an important basic question. The latter is estimated to be about 2–4 eV. Thus for the larger values of U ($\geqslant$5 eV) one is definitely in the strong correlation regime $U \gg zt$, while for the smaller values, mean field approaches to the effect of U and consequent independent electron-like theories may be adequate (extrapolating from experience with the orbitally nondegenerate Hubbard lattice model). Experimentally, $LaMnO_3$ above the 780 K transition (in the phase with no magnetic or structural long-range order) is an insulator, i.e. it is a Mott insulator. In tune with this, with the correlation energy systematics in such compounds (as inferred e.g. from core photoemission spectra), and the broad consensus in the field, I take U to be large, of order 5 eV or more. The U term can be written

$$H_U = U \sum_i n_i(n_i - 1). \tag{4}$$

Thus the total Hamiltonian of a collection of Mn e_g electrons on a lattice (two orbitals per site) consists of intersite hopping given by equation (1), Hund's rule coupling equation (2), Jahn–Teller coupling as well as related phonons (equation (3)) and finally Mott–Hubbard correlation U (equation (4)). It is thus given by

$$H = H_K + H_{Hund} + H_{JT} + H_{ph} + H_U. \tag{5}$$

There are several additional interactions and physical parameters which may be significant in different contexts. One is strain, which seriously influences the energetics of correlated octahedral tilts and distortions, with the corner-sharing constraint. A manifestation of this correlation is the 'antiferro' relation between the nearest-neighbour JT distortions so that the local and global strain is small. Such interactions have been discussed extensively [46]. In addition, there can be direct correlation between orbital states and between JT displacements on nearest-neighbour sites [27]. There is also the octahedron breathing mode coupled to the total number of e_g electrons on a site irrespective of its orbital distribution. One qualitative consequence of it might be the observed steep decrease in the JT ordering temperature with doping; the added holes induce breathing-mode distortions which disorder the antiferro distortive arrangement of the Jahn–Teller polarons [36]. The effect of long-range Coulomb interaction between the e_g electrons and the Re and Ak ions is also ignored (see section 3 and references there for a discussion of this).

Disorder has major effects on the observed properties of manganites [47]; that due to doping is nearly unavoidable. This is exemplified in the problem of A-site disorder, inevitable unless the dopants are ordered as has been achieved in $La_{0.5}Ba_{0.5}MnO_3$ [47]. It is known that in case of this system, the physical properties, and indeed the phases, are very different depending on A-site order [6, 47, 48]. One necessarily has ion size and charge variation on an atomic scale which has direct electronic effects. The ion size can also act via strain, for example. Experimentally, two classes of well-known consequences are the following: local ion size fluctuation, for a general incommensurate doping x, strongly reduces the Curie temperature T_c [49]. Attfield and collaborators [49] found that T_c decreases linearly (down to less than half its 'uniform' value) with the rms variation in ion radius, assuming that ions are distributed completely randomly on each site. Tokura and others have shown [6, 47, 48] that for a given composition x near $(1/2)$, the relative sizes of the Re and Ak ions (both of which occupy the A site of the ABO_3 or perovskite structure) determine whether the low-temperature phase is orbitally ordered or only magnetically and the nature of the phase above the ordering temperature. There are in addition effects due for example to deliberately introduced disorder, as with Al substituting randomly for Mn in $La_{1-x}Sr_xMnO_3$ [50], relatively long-range strain randomness due to surfaces, interfaces, cracks, strain fields associated with small defects, etc.

The effects are large, and are clearly associated with the observed high sensitivity of physical properties to perturbations.

2. Models and their consequences

Given the complexity of the problem, theoretical models for manganites focus on one or more of the above interactions as crucial, and develop approximate theories whose results resemble some experimental features of manganites. We mention briefly here a few classes of theories, and then describe the microscopic two-fluid (lb) model developed by us. The consequences of the latter are described in the next section. It is broadly accepted that in addition to double exchange, electron–phonon coupling is very significant. Indeed, manganites can be viewed as a 'laboratory for electron–phonon physics' [39].

2.1. Ab initio electronic structure

The electronic, magnetic and structural properties of manganites have been actively explored for more than a decade using a variety of theoretical *ab initio* methods for electron dynamics in solids, e.g. Hartree–Fock [51], local density approximation or LDA [25, 27], local spin density or LSD [24, 26] without and with [28] self-interaction, LDA + U [27, 29, 30]. An *ab initio* approach for this family poses well-known special challenges such as the following. These systems have (unfilled d shell) electrons with strong Coulomb interactions rather than quasi-independent ones for which conventional band theory is most reliable. There is a variety of phases with energies very close to each other. Nonzero temperature behaviour of doped nonstoichiometric disordered compounds is of interest often while most accurate calculations can be done for ordered stoichiometric compounds at $T = 0$; the difference can be quite radical. In spite of these limitations, the calculations are essential for several reasons. They constitute the base of our theoretical understanding in many cases and it is through them that one arrives at values for the sizes of the necessary ingredients for a realistic model (e.g. interactions and Hamiltonian parameters). I illustrate these general comments now in the context of manganites.

All electronic structure calculations agree broadly with the picture described above of crystal field split e_g and t_{2g} states. The band of electronic states near the Fermi level is e_g like, while the one identifiable with t_{2g} states is well below the Fermi level, as is the oxygen p band. There is clear evidence for large on-site inter-d-orbital Coulomb repulsion leading to a large Hund's rule-like ferromagnetic exchange coupling J_H. Further, cluster calculations, constrained electron occupation number estimations of U [25] and interpretation of photoemission experiments [44] all point to large U, in the range 5–10 eV, while the bandwidth is 2–4 eV. The naturalness and the importance of Jahn–Teller-like distortions are also explicitly brought out.

The properties of the parent $LaMnO_3$ compound as obtained from various *ab initio* approaches are quite illuminating. Approximations which neglect U lead to either a metal, or to an AF insulator with a relatively small gap and a small JT distortion Q_0. There is a synergistic effect between U and Q_0; on including the former, one obtains a phase similar in properties to that observed, with large distortion Q_0. With pressure, it is seen experimentally [52] that the JT distortion of the unit cell decreases continuously and vanishes at about 18 GPa. However, the resistivity continues to be insulating, and becomes metallic only above 32 GPa; this intervening phase could be a Mott insulator, not a band one. Detailed recent calculations (LDA + U, LDA + DMFT) [30] on the other hand suggest that this phase is likely to be an insulator because of as yet unobserved small long-range distortions present in addition to large U. Such a conclusion points to a limitation of this kind of approach in directly confronting experiment. For example, the experiments could imply that at intermediate pressures there is a Jahn–Teller

liquid phase with no long-range order, but short-range order, of the sort found at zero pressure but above the JT ordering temperature [34]. Such a liquid phase is not realistically accessible to *ab initio* calculations.

The electronic structure results provide estimates for parameters for simplified models of the sort mainly discussed here. The numbers have been quoted earlier. Additionally, authors have developed and used tight-binding as well as Jahn–Teller coupling parameterizations to fit the *ab initio* results. Two examples are the use of a model very similar to equation (6) in [29] and [30], and the exploration of cooperative Jahn–Teller effects in [27].

2.2. Strong Hund's rule coupling J_H only, or double exchange

As pointed out above, there is a strong effectively ferromagnetic coupling $J_{\rm H}$ between t_{2g} spins and e_g electrons on the same site. Thus when an e_g electron hops from one site to the next and the associated t_{2g} spins do not point in the same direction, the effective hopping amplitude is the bare one times the spin overlap factor because of the large $J_{\rm H}$; the latter is $\cos(\theta_{ij}/2)$, where θ_{ij} is the angle between the classical t_{2g} spins at i and j, assumed to fixed length vectors [33]. This double exchange (DE) mechanism leads simultaneously to ferromagnetism and metallicity in doped manganites. Further, at a given doping, as the temperature increases and t_{2g} spins disorder thermally, the average kinetic energy of the e_g electrons decreases and their incoherence increases. One thus expects a strong correlation between metallicity and the ferromagnetic–paramagnetic or Curie transition, which is observed. By the same token, application of a magnetic field near $T_{\rm c}$ polarizes the t_{2g} spins and should increase the e_g electron mobility or current. For these qualitative reasons, it is generally believed that double exchange explains colossal magnetoresistance (in a generic doping regime) as well as the association of the insulator–metal transition with the paramagnetic–ferromagnetic transition. The most detailed early calculations in the double exchange model (which cannot be solved exactly) are those of Furukawa [53], who used single-site dynamical mean field theory (DMFT), and obtained self-consistently the local magnetization and the time-dependent on-site self-energy of the e_g electron, which can be done exactly for infinite dimensions [54]. This nonperturbative method is known to be accurate for strong interaction phenomena in which spatial correlations do not play a critical role; it is expected to work well here in the absence of orbital order, etc. One finds a Curie transition, but to an incoherent metal, not an insulator. This approach leads, for example, to a nearly completely incoherent paramagnetic metal becoming a metallic ferromagnet below $T_{\rm c}$ as happens for LSMO, the most metallic of the manganites. However, even for this system, there are several major differences between theory and experiment. Some are mentioned below as part of the shortcomings of the pure DE model. They imply that other interactions are qualitatively important.

Some doped manganites are insulating paramagnets with a Curie transition to a metal or to an insulator. Almost all manganites have, for low doping, an *insulating* ferromagnetic ground state. Now, in a DE model, the only generic way a doped manganite can avoid being metallic is via Anderson localization of electronic states near the Fermi energy, this arising from e_g electron motion in a disordered background of t_{2g} spins. Careful calculations [55] show that the fraction of states localized thus is very small; for example, at $x \sim 0.25$ or so, only about 0.5% of the e_g states are localized with the maximum possible disorder of t_{2g} spins. Secondly, Millis and co-workers [41, 42] pointed out that the large changes in electrical resistivity observed near $T_{\rm c}$ cannot be understood in a pure spin disorder picture and that the effect of strong electron lattice coupling leading to Jahn–Teller polaron formation must be included. This is also supported by a large body of experimental evidence for polarons. Short-range and long-range orbital order may require additional ingredients. There are also other spin interactions present, e.g. the superexchange between t_{2g} spins which can be antiferromagnetic

or even ferromagnetic, depending on the relevant e_g orbital configurations, and a ferromagnetic virtual double exchange which is possible when a JT polaronic site and a hole are nearest neighbours (see [56, 57, 59] and section 3 below). Competition between antiferromagnetism and DE ferromagnetic exchange, leading to possible phase separation when frustrated and amplified by disorder, has been suggested by Dagotto and co-workers (see e.g. [5, 9]) to be the cause of the ubiquitous two-'phase' coexistence phenomenon in manganites. We [56–59] have argued that at least for $x < 0.4$ the ferromagnetism observed in manganites arises overwhelmingly from virtual double exchange which is of second order in the hopping, (see [56, 57, 59] as well as equation (8) and the discussion there) rather than double exchange which is linear in it.

2.3. Strong Hund's rule coupling J_H and Jahn–Teller interaction g

As mentioned above, Millis and co-workers [41, 42] showed that it is essential to include the effect of the strong coupling of the twofold degenerate e_g orbitals to the octahedral symmetry-breaking Jahn–Teller lattice modes. The static distortion induced by this coupling produces a polaron, lower in energy by E_{JT}. Using single-site DMFT, they determined self-consistently the on-site polaronic distortion, the self-energy of the e_g electron and the mean field magnetization. In addition to such equilibrium quantities, transport properties were calculated. They found for the 'half-filled' case (i.e. $n = 1$ or $x = 0$) that at high temperatures, i.e. temperatures above T_c, there are large polaronic distortions which diminish and disappear below T_c. The (second-order) Curie transition can be a metal–insulator transition. This is suggested to be a general feature of manganites even away from $x = 0$, e.g. doped ones. One feature of the calculation noted by the authors is that away from half-filling (i.e. for nonzero doping x), the Curie transition is either from a metal to a metal (for not too large g) or from an insulator to an insulator (for large g); there is no insulator to metal transition, unlike what is commonly seen experimentally. The effects (of temperature, magnetic field, etc) are in general smaller. Correlation U and coupling to breathing mode distortion will tend to reduce the difference in results for the doped and undoped systems, as pointed out by the authors.

Two approximations seem to be crucial; one is that in the adiabatic regime, i.e. for small γ, the static limit ($\gamma = 0$) is not only a good approximation for the physical properties, but additionally the effects of nonzero γ are obtainable *perturbatively* (and therefore negligible for small γ) even for the large electron lattice coupling λ present in these systems. The second is that one is not in the strong correlation ($U > zt$) regime, and that therefore there are no qualitative strong correlation effects. The first approximation is one of the major questions in electron–phonon physics (see e.g. section 5.2 below). For large λ, it is possible that the small parameter is not γ but $\eta = \exp(-\lambda/\gamma) \ll 1$. The factor arises from phonon dynamics and is not perturbative in γ. It (η) controls the effective amplitude for polaron hopping and thus the bandwidth; for $\eta \ll 1$, the polaron is essentially site localized, whereas the conclusion from the $\gamma = 0$ limit would be that the states form a broad band with the width determined by the bare hopping broadened further by static disorder scattering. The contrasting local (l) polaron (and coexisting b or band electron) idea is developed in [56–60] and briefly described below (section 3). A one-orbital Holstein model including dynamical effects has been extensively investigated by Edwards and collaborators [61]. Early work exploring dynamical polaron effects in the Holstein model and applied to manganites is due to Roder, Zang and Bishop [62].

2.4. Strong Hund's rule coupling J_H and strong correlation U

There is a large body of theory [63] in which the manganite is treated as an orbitally twofold degenerate electron system with strong Hund's rule coupling J_H (and hence double exchange)

as well as large correlation repulsion U. Ideas developed in the context of strong correlation approaches to the high-T_c cuprates are often used. Orbital liquid, orbital long-range order, and various magnetic phases have been explored. Polaronic effects are absent by choice (essentially, g is assumed to be small enough to be qualitatively unimportant). There are no metal–insulator transitions at general doping.

2.5. Computer simulation

The complexity of the manganite family and the variety of interactions (some mentioned above in section 1) naturally suggest numerical approaches for modelling their behaviour. I do not describe this large effort, but mention one illustrative contribution, namely attempts to understand inhomogeneities on micron scales present in several manganites [5, 9]. Dagotto and co-workers have argued that this is frustrated phase separation. If the system is such that one has two phases with a discontinuous transition between them such that for some parameter (say a coupling constant) they are equal or very nearly so in free energy, small fluctuations of this parameter are observed (in simulations on some model systems) to produce large regions of one phase or another. The simulations performed [64] were of frustrated square lattice Ising spin models with competing interactions, and an additional interaction chosen to produce a first-order transition. Correlated disorder, e.g. in a random field Ising model with long-range nonlocal effect of the random magnetic field, is argued to mimic the propagation of inevitable local size disorder effects in doped manganites through lattice strain. This was shown to continue to cause similar phase separation effects in higher (three) dimensions [65]. The random-field Ising model itself describes two macroscopic 'states' that are degenerate in the absence of a magnetic field, and the random field mimics random local preferences for one or the other of the two. Manganites are assumed to have, for certain conditions of doping and chemical identity, etc, two energetically competing phases which are however distinct enough in the nature of their order that there is a discontinuous transition between them. The above-mentioned dopant caused inevitable disorder, and its long-range, elastic strain-generated effect is argued to produce sizeable domains of the two phases; the system is homogeneous however in composition or electrical charge density. If the two 'phases' are insulating and metallic respectively, and the domains are large, electrical transport can be modelled classically. A simple approach is via a resistor network (e.g. classical percolation theory [66]). Further, if the two regions are identified as having, respectively, antiferromagnetic and ferromagnetic coupling, statistical mechanical simulation can lead to a strongly peaked temperature-dependent resistivity. A magnetic field will affect the ferromagnetic domains substantially if these are already large, leading to a colossal reduction in resistivity. This is a mechanism for colossal magnetoresistance. An analytical Ginzburg–Landau approach to the bicritical regime, and the effect of an external magnetic field in enhancing fluctuations tracked by renormalization group methods, have been discussed by Murakami and Nagaosa [67].

The proposal mentioned above for CMR may be appropriate for certain physical and chemical conditions in manganites (e.g. doping, ion size distribution). Indeed, experimentally, the prominent A-site disorder effects in half-doped manganites strongly suggest that this could be the case [6, 47, 48]. It seems, however, that the ubiquitous occurrence of CMR in a wide incommensurate doping range (as mentioned earlier; see also [3, 4, 6–8, 10]) requires other ideas, some of which are mentioned in this review. The possible existence of more than one kind of CMR in the manganites is clearly indicated.

2.6. The lb model

The two e_g electrons per site model described by equation (5) above is already too complicated to be investigated directly, even numerically for sizeable finite systems (for an N-site system

with two orbital and two spin states at each site, ignoring the lattice degrees of freedom, there are 16^N states in different orbitals at each site). The low energy states of the system when g is large are described by the two fluid lb model proposed and explored by us [56–60]. The former, namely l, has site energy $-E_{\rm JT}$ and has an exponentially reduced hopping amplitude t^* to the nearest neighbour b site, while the latter (b) has energy zero on sites where the l particle is not present and a very large energy $U(\sim\infty)$ on l sites, with an undiminished hopping amplitude t to b states on the nearest neighbour sites. The total number of l and b electrons together is of course constrained to be $(1-x)$ per site; further, the two species are in equilibrium, namely they have the same chemical potential. Since g is large in manganites, the lb model is a realistic simplification. Our results have been so far for $t^*=0$. The l polarons are static and site localized. In this limit, for the orbital fluid regime, i.e. for the large region of doping and temperature without long-range orbital order, the single site DMFT approach we have used is appropriate since statistically, every site is like every other. The results obtained have been compared with observations, and explain them qualitatively and quantitatively.

Large nanoscopic electronic inhomogeneity is outside the single site DMFT approach. It is simulated numerically using the lb Hamiltonian with an additional term describing electrostatic Coulomb interactions involving charged l and b particles (e.g. section 3.2). I briefly motivate the lb model starting from the standard tight binding, one d band model with twofold degenerate e_g orbitals per site (a more detailed discussion is given in [57]) and then describe some results. The strong electron–lattice coupling (large Jahn–Teller lattice distortion) leads to the natural reorganization of the initially doubly degenerate e_g orbital state at a lattice site into two states, one for which the minimum of the lattice potential energy is at Q_0, namely a Jahn–Teller small polaron, and another for which the lattice potential energy is a minimum at zero displacement; this state is therefore nonpolaronic. An electron at site i can be in one of these two states, labelled l and b respectively, with the former having a site energy lower by $2E_{\rm JT}$ compared to the latter ($E_{\rm JT}$ below the original degenerate level energy). Their hopping behaviour, namely kinetic energy, is very different. The l polaron hopping amplitude is reduced exponentially by the 'polaronic' or Huang–Rhys [68] factor $\exp\{-(E_{\rm JT}/\hbar\omega)\} = \exp\{-(\lambda/\gamma)\} = \eta \sim \exp\{-(5\text{ to }10)\}$, this being broadly due to the overlap between the initial and final phonon states at site i. We argue that this exponential narrowing of the l bandwidth occurs for strong electron–phonon coupling $\lambda > 1$ even in the adiabatic regime $\gamma < 1$, provided that $(\lambda/\gamma) \gg 1$, as is the case for manganites (for these, $\lambda \sim$ 1–5, and $\gamma \sim$ 0.2–0.3). A calculation [69] for the one orbital per site Holstein lattice polaron model (with $U=0$, and using the Lang–Firsov transformation [70]) estimates the leading perturbative or phonon fluctuation correction to the 'mean field' reduction factor η to be of relative order $(t\eta/\hbar\omega_0) \ll 1$. There is no such reduction in the b electron hopping amplitude. By contrast, in theories for manganites which include the effect of strong electron lattice (Jahn–Teller) coupling, one either assumes that the classical Jahn–Teller distortion results have negligible perturbative corrections because the adiabaticity parameter γ is small [41, 42], or that the quantum phonon effects act equally on both the states [71]. Though the lb model is naturally viewed as a limiting case of the tight binding two e_g orbital per site system, the model itself has no reference to two orbital states per site; the low energy sector describes two coexisting fermionic fluids, one site localized (l) and the other (b) with undiminished intersite hopping, but to be found only on sites where the l fermions are not (for large U). The characteristic strong electron–phonon coupling effects are captured in a two-fluid Hamiltonian H_{lb}, whose simplest form is

$$H_{lb} = -E_{\rm JT}\sum_i l^+_{i\sigma}l_{i\sigma} - t\sum_{\langle ij\rangle} b^+_{i\sigma}b_{i\sigma} - \mu\sum_i (n_{li\sigma}+n_{bi\sigma}) + U\sum_i n_{li\sigma}n_{bi\sigma} - J_{\rm H}\sum_i (\mathbf{s}_{li}+\mathbf{s}_{bi})\cdot\mathbf{S}_i. \tag{6}$$

We notice that effects of *all* the three strong local interactions are still present in the above Hamiltonian. Effectively, the large electron–lattice coupling g leads to two distinct effective fermionic species or fluids, l and b. The former is a JT polaron, essentially site localized, with a lowered energy $-E_{\rm JT}$. The latter is a band electron, hopping from site to site in a random medium which has zero site energy on hole sites and large repulsive energy U (which is composed of the Mott–Hubbard correlation U^* and the 'anti-Jahn–Teller' state energy $E_{\rm JT}$) on l polaron sites. The e_g spins on site i have a strong Hund's rule ferromagnetic coupling $J_{\rm H}$ with t_{2g} spins at the same site. The number of electrons per site in the system is $(1-x)$ on the average: this is the total number of l polarons and b electrons. We discuss these results in section 3, and the nature of l polarons and their coexistence with band b electrons in section 5.

Some further approximations have already been made in writing the above Hamiltonian. First, we neglect the intersite hopping of l polarons, which is nonzero though exponentially small. In particular, we ignore the largest such term, of amplitude $\sim t\eta$, which arises from the hopping of the l polaron to the nearest-neighbour b state; this hybridization is the dynamical cause of internal equilibration of the lb system. We assume that there is such an internal thermodynamic equilibrium, namely that the $(1-x)$ electrons on the average per site are distributed among the l and b states, i.e.

$$\langle n_l \rangle + \langle n_b \rangle = (1-x) \tag{7}$$

with a common chemical potential μ. These constraints determine, (for a given x, $E_{\rm JT}$, t, and T) the relative number of l polarons and b electrons. One consequence of neglecting lb hybridization is that equation (6) does not describe the physics of electron coherence that occurs below $T^* \sim (\eta t/k_{\rm B}) \sim 100$–$150$ K, e.g. the dynamic nature of the l polaron, the band-like behaviour of the system, the dramatic decrease of the electrical resistivity as T decreases well below $T_{\rm c}$, its T^2 behaviour at low temperatures and the relatively small residual resistivity at $T = 0$. We develop low-energy theories here which are accurate for temperature/energy scales higher than T^* and compare with a large number of experiments in this regime. Our calculations of those low-temperature properties that depend on electron coherence which can develop in the metallic regime ($0.2 < x < 0.4$), e.g. electrical resistivity and Hall effect, are not reliable. On the other hand, properties such as the ground state energy are not very much affected; for example, inclusion of intersite l polaron hopping is expected to shift the critical concentration $x_{\rm c}$ for the insulator–metal transition downwards by at most a few per cent. The intersite lb hybridization is easily included by adding the relevant term to H_{lb} in equation (6).

The second approximation (in a picture where the lb model is derived from a two e_g orbital per site Hamiltonian) is that though the actual intersite hopping matrix element of the b electron depends on the angles θ_i and θ_j describing the exact admixture of the two e_g orbital basis states, we effectively integrate out this degree of freedom, i.e. the hopping is represented by a single amplitude, which is the statistically and quantum mechanically averaged effective hopping amplitude for the b electron. Clearly, this is sensible in the orbital fluid regime, where there is no frozen long-range order of the orbitals. In the orbital glass regime as well, the hopping amplitude t of the b electrons is the average over the frozen (l polaron) configurations (angles), and we neglect any specific effects of fluctuations with respect to this average. Again, equation (6) can be augmented easily with such explicitly orbital state dependent terms if necessary.

The low-energy sector of the lb Hamiltonian H_{lb} (equation (6)) is the lower Hund–Hubbard band, for large $J_{\rm H}$ and large U. This is the sector we focus on for comparison with appropriate physical properties. We are thus interested only in those e_g (or b electron) states which point along the local t_{2g} spin direction, and have single (or zero) occupancy on any site. Often one works in the $J_{\rm H}, U = \infty$ limit, so only the lower Hund–Hubbard band has finite energy;

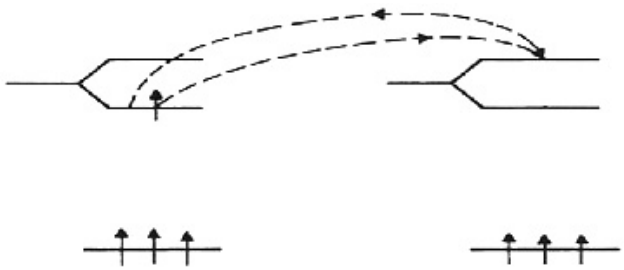

Figure 3. Schematic illustration of second-order virtual nearest-neighbour hopping process leading to a ferromagnetic t_{2g} spin coupling.

because J_H and U are large in relation to t, detailed calculations show that the $J_H, U = \infty$ limit is quite accurate. Because of this focus, in the $x = 0$ limit (e.g. the $LaMnO_3$ end) the insulating state found in the lb model has a large Hund–Hubbard gap; in reality there could be other unoccupied bands in this gap, so the actual activation energy for electrical conduction is smaller. In the lower Hund–Hubbard band, there is a maximum of one l state and x b states per site.

The l polaron is a good excitation for energies smaller than the polaron (binding) energy E_{JT}. In an effective low-energy theory (for energy $<E_{JT}$), one integrates out states with energy larger than E_{JT}. This leads to at least one new virtual double exchange interaction which is *ferromagnetic*. The interaction, second order in t_{ij}, is illustrated in figure 3. It arises when an l polaron site and a hole site are nearest neighbours i and j, and the l electron (*not* the polaron) hops quickly from site i to site j and hops back, before the lattice distortion at site i relaxes, the timescale for the latter being about $(\hbar\omega_0)^{-1}$ or less. The energy of the intermediate lattice distorted state is $2E_{JT}$. The intersite hopping matrix element depends on the angle between t_{2g} spins at i and j, because of the strong on-site Hund's rule coupling between t_{2g} and e_g spins. For $J_H = \infty$ and classical t_{2g} spins, this interaction term is, in the orbital fluid regime, given by

$$H_{VDE} \sim -(t^2/2E_{JT}S^2)\sum_{\langle ij\rangle}\mathbf{S}_i\cdot\mathbf{S}_j[n_i(1-n_j)+n_j(1-n_i)] \tag{8a}$$

$$J^F = -(t^2/2E_{JT}S^2)x(1-x)\sum_{\langle ij\rangle}\mathbf{S}_i\cdot\mathbf{S}_j \tag{8b}$$

where one has averaged over the orbital directions at sites i and j in equation (8*a*) and further over the l occupations in equation (8*b*). This superexchange type of virtual double exchange coupling, second order in hopping, is ferromagnetic between the t_{2g} spins because of the Hund's rule, unlike the well-known Kramers–Anderson superexchange for electron spins in nondegenerate orbitals which is antiferromagnetic. It involves virtual hopping, unlike the double exchange which involves real hopping, and is thus linear in t_{ij}. We find that J^F_{ij} has the right size and x dependence, and that, for $0.2 < x < 0.4$, it is by far the more significant magnetic interaction than double exchange because the latter is due to the hopping of b electrons which are small in number in this x range. We estimate J^F_{ij} to be about 2–3 meV. The interesting connection between charge (orbital) and spin degrees of freedom implied by equation (8*a*) and its intrinsically random nature have not been explored, but are quite likely connected with the A-site disorder [6, 47, 48] and Griffiths phase [72] effects observed. Recently, several pieces of evidence supporting the above origin of intersite ferromagnetic spin coupling in manganites have turned up. From an analysis of the EXAFS lineshape in terms of the mean square spread of Mn–O bond lengths, and the temperature/doping dependence of the latter, it was inferred [73] that holes are strongly correlated with JT distorted sites as nearest neighbours; it is argued that the corresponding spins exist as ferromagnetic pairs.

Considerable paramagnetic susceptibility evidence [74] points to Curie constants appropriate to nearest-neighbour magnetic pairs of ferromagnetically coupled $S = 2$ and $S = (3/2)$ spins, i.e. Mn^{3+} and Mn^{4+}.

The antiferromagnetic state of the two end members of the series, namely for $x = 0$ and for $x = 1$, means that there is an antiferromagnetic coupling between t_{2g} spins. This is most naturally via Kramers–Anderson superexchange as discussed for example in [31]. The results show for example that both the size and sign of the superexchange depend on the occupied nearest-neighbour (nn) e_g orbital states. One can rationalize for example the occurrence of A-type AF order for $x = 1$; in the ab plane the nn e_g orbitals are 'antiferro' correlated, so the t_{2g} spin coupling is ferromagnetic, while in the c direction the 'ferro' correlation of the orbitals leads to an antiferromagnetic spin coupling. This is indeed observed. The nn AF coupling is of the usual form,

$$J_{ij}^{\mathrm{AF}} = -J\mathbf{S}i \cdot \mathbf{S}_j. \tag{9}$$

3. Results of the strong correlation, two-fluid model

I outline here some results obtained for the properties of manganites modelled as two coexisting fermionic fluids, one polaronic and heavy, and the other nonpolaronic and light [56–60].

The two-fluid model above is formally akin to the Falicov–Kimball model for a system of correlated f electrons and coexisting band spd electrons which was developed in the context of rare-earth metals and alloys, and has been investigated extensively [75]. The presence of spin degrees of freedom of the t_{2g} spins and the e_g electrons is a qualitative difference.

3.1. Orbital fluid

The strong coupling approach used by us to understand the low-energy behaviour of the lb model in the form of equation (6) is the dynamical mean field theory (DMFT) [54]. In the single-site DMFT (or self-consistent impurity model) we work with, the b electron at a given site sees a bath of electrons with which it hybridizes (hybridization amplitude $V(\varepsilon)$ at energy ε). The l polaron has a site energy $-E_{\mathrm{JT}}$. The local spin experiences a molecular field $\mathbf{\Omega}$, which is the average effect of all other spins. Thus the DMFT Hamiltonian can be written as

$$\begin{aligned} H_{\mathrm{DMFT}} = &-E_{\mathrm{JT}} n_l - \sum_{\langle k\sigma\rangle} V(\varepsilon_k)[b_\sigma^+ c_{k\sigma} + c_{k\sigma}^+] \\ &+ \sum_{\langle k\sigma\rangle} \varepsilon_k c_{k\sigma}^+ c_{k\sigma} - \mu(n_l + n_b) + U n_{l\sigma} n_{b\sigma} - J_{\mathrm{H}}(\mathbf{s}_l + \mathbf{s}_b) \cdot \mathbf{\Omega} \end{aligned} \tag{10}$$

where $V(\varepsilon)$, μ, and $\mathbf{\Omega}$ (or rather the probability $P(\Omega)$ and the resulting average magnetization m) are determined self-consistently for a given temperature T, doping x and Hamiltonian parameters. Results for the l and b spectral densities at representative dopings and temperatures are shown in figure 4.

At $T = 0$, the DMFT can be solved exactly [56, 57, 59] in the J_{H}, $U = \infty$ limit, which is actually a very good approximation. The effective b bandwidth goes as $\sim\sqrt{x}$ for small x (essentially because of strong correlation U induced b exclusion), so that the b band is relatively narrow for small x. The band bottom for small x can thus lie above $-E_{\mathrm{JT}}$, which is very nearly the chemical potential, so there are no occupied or low-energy b (extended) states: only localized or easily localized polaronic states are occupied, and the ground state is a ferromagnetic insulating dense polaron liquid in the DMFT (figure 4(a)). The system is most likely a ferromagnetic polaron glass in reality because of the pinning of l polarons by even weak random potentials, e.g. Coulomb interactions, as found for example in realistic computer

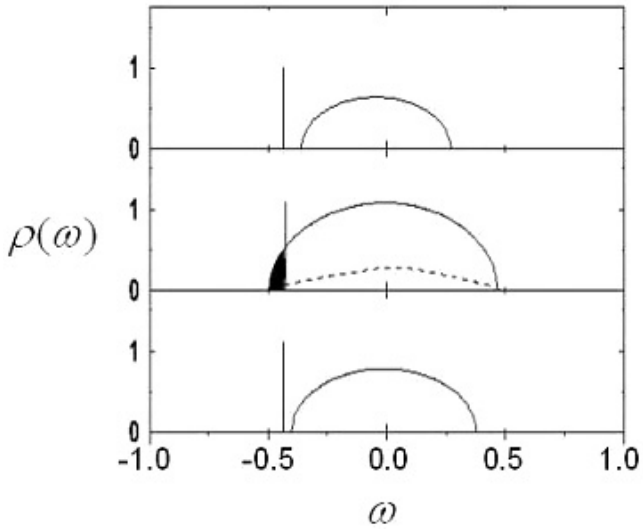

Figure 4. Spectral densities in the single-site DMFT solution of the *lb* model [56, 59]. The three graphs, namely top, middle and bottom, are referred to as *a*, *b* and *c* respectively in the text. The *l* level, and the *b* (band electron) spectral density (*y* axis) are shown in units of the bare semicircular density of states (*x* axis), for various dopings *x* and temperature *T*. The Jahn–Teller energy $E_{\rm JT}$ is 0.5 in these units. The model parameters are $2D_0 = 2.4$ eV, $E_{\rm JT} = 0.5$ eV, $U = 5$ eV, and the virtual double exchange ferromagnetic coupling is 2.2 meV.

simulations (see figure 7 and discussion there). There are also intersite orbital or polaronic correlations, explicit or induced (the latter for example via coupling to strain, or via admixture with *b* states on neighbouring sites); these can give rise to short-range or even long-range orbital/polaronic order. Qualitatively, the insulating ferromagnetic ground state found here for small doping (generic to manganites, but difficult to obtain in most models) is for two reasons. First, the ferromagnetic virtual double exchange coupling equation (8) requires only that there be JT polarons and holes next to each other. The latter can be localized (the former, of course, are site localized) so that the system can be insulating in contrast to the double exchange model where the ferromagnetic exchange is due to mobile holes or to metallicity. Second, the system consists actually of only a small concentration *x* of holes doped into $LaMnO_3$ which is known to be a polaron crystal, so the density of polarons can be expected to be high, about $(1 - x)$ per site; the other (b) electrons move in a medium with a very small concentration (x) of favourable sites (with a concentration below the percolation threshold p_c), avoiding polaronic sites, so their overall kinetic energy gain is smaller than the Jahn–Teller energy loss. Disorder adds crucially to this picture. Inevitable dopant disorder and the associated Coulomb interaction energy can freeze or pin the *l* polarons and lead to strong nanoscopic electronic inhomogeneities, as shown in computer simulations of the *lb* model including such interactions (see section 3.2 below).

As doping increases, the effective bandwidth of the *b* electrons increases and there is *b* spectral density below $-E_{\rm JT}$ (the chemical potential continues to be close to it), so extended states are occupied and the system is a ferromagnetic metal (e.g. figure 4(b)). Thus, with increasing doping, there is a $T = 0$ insulator to metal transition (the critical concentration x_c for this is in the observed range 0.2 for typical parameter values). This, and the insulating ferromagnetic ground state for small *x* described above, are two characteristic manganite phenomena which are simply understood in the two-fluid model. The DMFT calculations show in detail how they depend on various material parameters.

In the metallic state, electron transport is by the mobile b electrons which we find to be small in density, $\ll x$. The density of JT polarons is high. They are necessarily dynamic because of for example intersite lb hybridization, an energetically small effect neglected in the simplest version equation (6) of the lb model and in the DMFT. This process is expected to reduce their number density also self-consistently. As the temperature increases at a given doping, the effective mobile electron (b) bandwidth decreases because of the t_{2g} spin disorder and the strong Hund's rule coupling J_H. Consequently, the number of occupied b states decreases dramatically, and one can have an insulator (figure 4(c)). We have also calculated the total electrical resistivity solely from the b electron propagators (this can be done in $d = \infty$ where the relevant vertex corrections vanish); the l polarons are immobile and do not transport charge. Some results are shown in figure 5. We find a clear thermal insulator–metal transition, nearly coincident with the Curie transition. Interestingly, the insulator-like temperature dependence of the resistivity in the paramagnetic phase leads to an activation energy (for the b carrier) which is close to what is observed in systems, e.g. LCMO and NdSMO, where such comparisons are possible [56, 59].

Depending essentially on the ratio δ of the Jahn–Teller energy E_{JT} to the bare electron half bandwidth D_0, the thermal transition can be from insulator to insulator (large δ) or from metal to metal (small δ) in close correspondence with experiments on manganites (figure 6). For example, the LSMO compounds are believed to have the widest bands; both the paramagnetic and the ferromagnetic states are metallic. In the narrow band system PCMO, both the phases are insulating, while in LCMO, which is believed to be intermediate, the Curie transition is from an insulator to a metal. There is strong neutron evidence that the transition is of first order [76]; this could be because of coupling to other degrees of freedom, e.g. strain, neglected in the lb model Hamiltonian equation (6), and in the DMFT calculation.

We also calculate the electrical resistivity in a magnetic field, which couples to the t_{2g} and e_g spins. We find a colossal decrease (figure 5). The physical reason is that the magnetic field increases the t_{2g} spin magnetization; the effect is strongest near T_c. As a result, because of the strong Hund's rule coupling, the b bandwidth goes up, so the b band bottom can go below the chemical potential and some extended b states can be occupied. The resistivity decreases dramatically. This can occur for *general* doping in an orbital liquid for reasons not connected with the critical value of a particular coupling constant or doping condition, bicriticality or disorder-enhanced two-'phase' coexistence [9]. Ours is a generic mechanism having to do finally with the coexistence of localized polaronic and extended electronic states at a microscopic level. This can happen for strong electron–phonon coupling and double degeneracy of the e_g orbital. Further, in a manganite, because of the strong Hund's rule coupling, an external magnetic field can influence the conditions of coexistence of the two. The effect is strong because the mobile carrier density depends exponentially on an activation-like energy which is affected directly by the magnetic field. It is present at arbitrary doping essentially because the polaron is strongly localized; the chemical potential is pinned at the polaron energy, so there is a large reservoir of electrons there.

A number of other consequences of the two-fluid model have been noted [57]. One is that the number density of b electrons is much smaller than x, the hole density, and decreases strongly with temperature on a scale of T_c. For example, at $x = 0.3$ in LCMO, $\langle n_b \rangle \leqslant 0.05$ [59]. This is connected with several puzzling observations. For example, the photoemission intensity, from the earliest measurements [77] to the latest ARPES data on layered manganites [78], imply that the density of electronic states at the Fermi level is unusually small. Optical conductivity $\sigma(\omega)$ measurements [79] yield a small Drude weight; the optical sum rule oscillator strength moreover decreases strongly with increasing temperature. The plasma frequency of doped LCMO is much lower than expected [80], corresponding to a

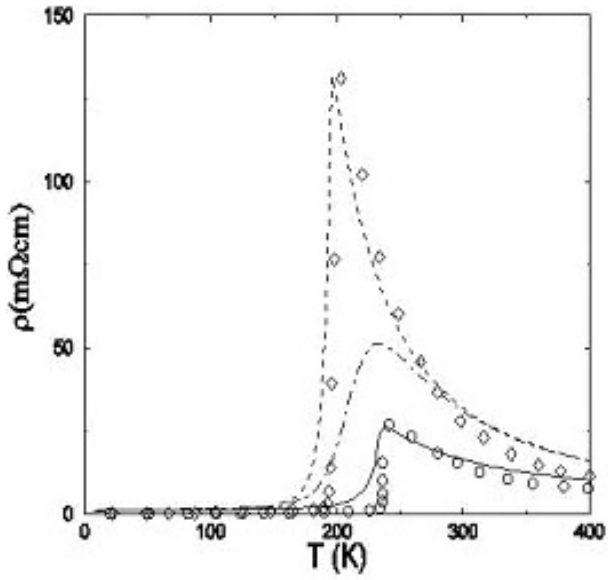

Figure 5. Resistivity (y axis) calculated in single-site DMFT versus temperature (x axis) for $E_{\rm JT} = 0.5$ eV, $U = 5$ eV and $x = 0.3$ [56, 59]. The bare bandwidth $2D_0$ is 2.3 eV for the dashed and dash–dotted lines ($H = 7$ T) and 2.1 eV for the full line. The diamonds are the data for NdSMO and the circles for LCMO.

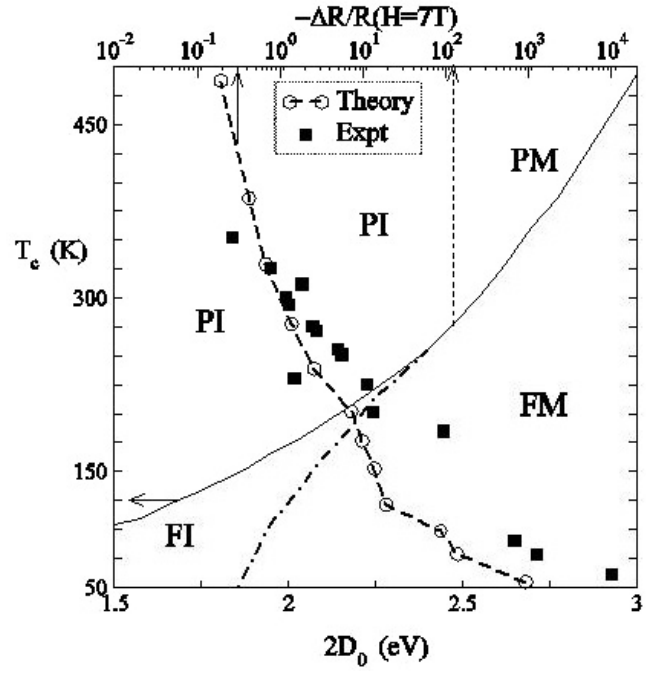

Figure 6. Materials systematics in the *lb* model [56, 59]. Ferromagnetic $T_{\rm c}$ versus bare bandwidth $2D_0$. The full line is the calculated $T_{\rm c}$ and the dash–dotted line separates the calculated ferro–insulator (FI) region from the ferro–metal (FM) region. The calculated and observed fractional resistance changes at 7 T are also shown.

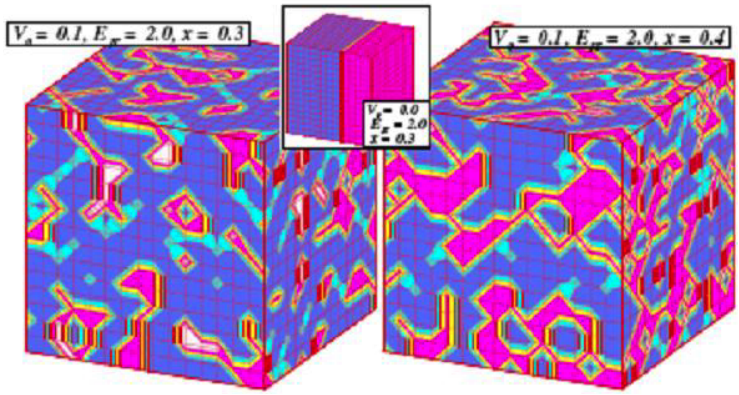

Figure 7. Real space electronic distribution obtained from simulations on a 16^3 cube. Magenta (darkest) denotes hole clumps with occupied b electrons, white (lightest) denotes hole clumps with no b electrons, cyan (second lightest) denotes singleton holes, and light blue (second darkest) represents regions with l polarons. The configuration on the left shows isolated clumps with occupied b electrons (b puddles). For larger doping, percolating clumps are obtained and the system is a metal (right). The inset shows results in the absence of long-range Coulomb interaction and shows macroscopic phase separation. All energy scales are in units of t.

free carrier density of about 0.04. All this can be rationalized if the carrier density probed in these experiments is identified with the b electron density. The l electron has an exponentially small quasiparticle weight at the Fermi energy; removal of the electron of a polaron by the photon actually shows up as a *mid-infrared* peak, centred at the polaron binding energy, whose contribution is excluded from the Drude weight. A comparison of $\langle n_b \rangle$ with the Drude weight in LSMO [79] is quantitatively successful both in absolute value and in temperature dependence, for a set of model lb parameters chosen to reproduce some other properties of the system (e.g. T_c, $\rho(T_c)$.[2] The large isotope effect on T_c can be rationalized in terms of the exponential dependence of the l polaron bandwidth reduction factor η on the inverse square root of the isotope mass. The l polaron contribution to T_c via double exchange is directly proportional to this bandwidth.

3.2. Coulomb interactions and the orbital glass

The lb model has been extended [82] to include electrostatic Coulomb interaction in the doped mixed valent manganites. It is apparent that, in its absence, the l polarons and the b electrons will phase separate, since then the b electrons gain maximum kinetic energy. However, including Coulomb interactions and imposing the equilibrium condition of the equality of *electro*chemical potential, one finds that macroscopic phase separation is muted to one of nanoscopic inhomogeneity with puddles of hole regions (home for b electrons) and regions of immobile l polarons. The scale of the inhomogeneity is set by the randomness of the dopant ions and the strength of Coulomb interactions setting a screening length scale of a few nanometres in the low-doping region. Figure 7 shows two examples of numerical simulation of the lb model equation (6) with the effect of additional Coulomb interactions included in the

[2] There are more recent measurements of $\sigma(\omega)$ which do not show a low-frequency Lorentzian or simple Drude form [81]. This could finally be due to l polaron coherence developing in these systems in the metallic phase as the temperature decreases. The effect of lb hybridization on b electrons, via a strongly temperature- and energy-dependent scattering, as well as absorption by dynamic polarons, is quite likely to change $\sigma(\omega)$ qualitatively. The earlier measurements, e.g. [79], could be under conditions such that because of pinning, l polaron coherence is absent in them.

Hartree approximation, for a 16^3 system with doping $x = 0.3$ and 0.4. The simulation is of the ground state for J_H, $U = \infty$. It is clear that the system is very inhomogeneous on a microscopic scale, though single phase on large length scales in the thermodynamic sense (insulating for $x = 0.3$ and percolatively metallic for $x = 0.4$ in figure 7). The intrinsic Coulomb disorder and consequent pinning are connected with the absence of heavy-fermion effects in the hybridized *lb* system, unlike rare-earth intermetallics, for example. The insulating regions are polaronic; if intersite correlations between them are included, the charge inhomogeneities do not change but short-range 'antiferro'-order naturally develops and the picture is very close to what is seen in STM experiments. Coulomb interaction as the cause of electronic inhomogeneities has been discussed for a long time, e.g. in connection with frustrated phase separation in the t–J model for cuprates [83], and in the context of the low-density 2DEG (droplet phases, [21]). It has been recently suggested [22] that in strongly correlated systems, two different phases (with different kinds of long-range order?) are likely to be close in energy; this is termed electronic softness. In such a case, ubiquitous long-range Coulomb or strain-related interaction can lead to strongly inhomogeneous states. While this scenario is plausible, our simulation addresses the question of electronic inhomogeneities microscopically, in a manifestly strongly correlated system. The two states are *not* distinguished by different kinds of order, but are quantum mechanically distinguished, by local energy and dynamics. In the presence of strong correlation (U in our case), there is a tendency for phase separation, which is restricted to nanoscopic scales by Coulomb interactions. The micron-scale inhomogeneities seen in a number of systems, e.g. via electron microscopy [15] or via position sensitive ARPES [15], are most likely due to other, elastic strain-related causes.

4. Current issues

Several open areas in manganite physics are also subjects of a great deal of current activity. Some have already been mentioned in earlier parts of this review. Examples are the role of A-site disorder in half-doped manganites (section 1.2), the possibility of different kinds of colossal magnetoresistance (sections 2.5, 3) and the overarching question of 'phase' separation (section 1.1). An area which is seeing high-quality experimental activity is that of ARPES experiments in bilayer manganites [78]. These show a pseudogap in the electronic density of states near the Fermi energy, resembling (in size, energy location, and most interestingly in angular dependence in the plane) that seen and well documented in underdoped cuprates.

5. Some questions arising

I conclude this review by mentioning two questions of broad interest raised by observations in manganites, both having to do with new physics that probably arises for strong electron–phonon coupling as doubtless present in manganites. The first is whether the strong electron–phonon coupling effects in them can be usefully described in terms of polarons, and if so of what kind? The second, related question, is the physics of strong electron–phonon coupling in adiabatic polaronic systems, namely systems in which $\lambda > 1$ and $\gamma < 1$, but $(\lambda/\gamma) \gg 1$.

5.1. Polarons

A large number of phenomena in manganites indicate the existence of polarons in them over a wide range of conditions; these composites of an electron and associated lattice distortion affect their physical properties fundamentally. In this subsection, I mention some of these phenomena and properties. Many of these have been discussed in terms of existing models for polarons, largely following the early work of Holstein [84] on an orbitally nondegenerate electron at a lattice site inducing displacement of an Einstein mode there. Whether one has polarons of this

kind or others more specific to the local symmetry and interactions in manganites, their number, correlation and dynamics, their role in the observed phenomena, and their direct observability are some of the major questions in the field as mentioned below.

As pointed out earlier, the twofold degeneracy of the e_g orbital of Mn is naturally removed by the Jahn–Teller effect, namely by breaking of its local octahedral symmetry since the coupling g between the e_g electron on-site and the $\mathbf{Q}_i$ modes (equation (3*a*)) is large ($g \sim 2$ eV A^{-1}). The composite of the e_g electron and the associated local lattice distortion is the Jahn–Teller polaron, widely believed to be present and most likely significant in manganites. (The local excess/deficit d electron density also induces a large breathing mode or uniform distortion of the octahedron of which the Mn ion is the centre; its consequences are not discussed here; the work of Narimanov and Varma [85] for example analyses manganite physics solely in terms of such polarons and mobile electrons.) I describe some observations argued to attest to existence of JT polarons and theories including the l polaron–b electron (two-fluid) model (see [56–60] and sections 2 and 3 above) used to describe phenomena in these systems.

Some relatively direct evidence for polarons in manganites follows from 'instantaneous' or short-time scattering experiments using pulsed high-energy neutrons or EXAFS, which determine pair distribution functions or PDFs [16–18]. The results show that in doped manganites, short and long Mn–O bond lengths exist on timescales over which the high-energy neutron or the x-ray traverses atomic (nanoscale) regions. The bimodal bond length distribution, most naturally interpreted as an appropriate Jahn–Teller distortion, is observed not only at or very close to zero doping, or at high temperatures, or in the insulating phase, but even in the most metallic of manganites, namely $La_{1-x}Sr_xMnO_3$ into the metallic regime, i.e. for $x > x_c$ and $T < T_c$. Signatures of local distortion are observed for conditions of doping and temperature such that there is no long-range lattice distortion generated superstructure (unlike in $LaMnO_3$ below 780 K); the system is pseudocubic. The decrease in the intensity of the bimodal distribution and in the bimodal dispersion with increasing x and with decreasing T [16, 18] suggests the following possibilities: (a) there are fewer Jahn–Teller polarons as x increases, (b) the polarons become dynamic progressively with decreasing T and increasing x, and (c) there is a decrease in the polaronic distortion. All these are likely to feed back on each other. In neutron scattering experiments, observations of diffuse scattering above T_c [86] have been described in terms of a polaron glass, i.e. a static arrangement of local JT polarons. At lower temperatures (e.g. below T_c, in the ferromagnetic metallic regime) this scattering becomes unobservably weak. Observations of the mid-infrared peak in optical conductivity $\sigma(\omega)$ [87], of nondispersive states about an eV or so below the Fermi energy in ARPES [88], and of local cubic symmetry-forbidden JT phonon lines in light scattering [37], have all been interpreted in terms of the presence of JT polarons. An assumption underlying these suggestions is that the conditions of small JT polaron formation are local (on-site), and are not therefore much affected (adversely) by doping and possible metallicity which gives rise to electrostatic screening. In the manganites, screening is poor, and the screening length scales are indeed larger than the unit cell size relevant for the kind of JT polaron formation mentioned above. However, polaronic signatures are feeble in the metallic, lower-T regime.

One simple well-known model is the Holstein polaron [84], corresponding to a tight-binding electron in an orbitally nondegenerate state on a lattice site couples strongly to a local Einstein phonon mode. It is well known that, in this model, the ground state for a single electron is extended for $g < g_c$ and is a self-trapped (Holstein) polaron for $g > g_c$, with a rapid crossover. It is assumed that the many-electron system will consist of either band electrons or of polarons, depending on g. In the latter case, it is believed (most obviously in the nonadiabatic regime) that the polarons form an exponentially narrow band at low

T, and at high temperatures hop incoherently from one site to another, surmounting (via coupling to thermal 'noise') the energy barrier associated with intermediate lattice displacement configurations. It has been argued, e.g. [4], that transport properties of manganites in the orbital fluid regime (approximately $0.2 < x < 0.4$), e.g. electrical resistivity ρ, Hall coefficient R_H and thermopower, can be understood this way. While Holstein polarons have been widely discussed [4] there is no investigation of the transferability of results for them to the rather different situation of manganites in which the tight-binding e_g electrons which can form polarons are orbitally twofold degenerate, can have high density, and other strong local correlations/interactions are present.

The other generic polaron model, namely the Frohlich model, arose for ionic solids, where an added electron produces long-range dipolar electrostatic distortion of the lattice. The importance of such polarons for manganites has been argued for by Alexandrov and co-workers [89].

As mentioned earlier above, Millis and co-workers [41, 42] pointed out the importance of local electron–phonon coupling in the context of manganites, namely for electrons in doubly degenerate e_g states. (They took the phonons to be classical, i.e. treated the lattice displacements as classical variables, with the statistical distribution of the JT distortion assumed to be the same at each site and determined self consistently). Because the phonons are treated classically, and the system has annealed disorder, the e_g electrons move in a static random medium. The polaron states form a band, further broadened by disorder. Millis *et al* found that the average polaronic distortion can be sizeable at high temperatures and decreases with cooling. The low-energy electronic states are organized into two lower Hund bands, one polaronic and another not, somewhat like the l and b states discussed above. The polaronic band is broader than the b band because of static disorder effects. In our two-fluid model the l polarons are also composite excitations of the orbitally twofold degenerate e_g electrons and JT lattice distortions. However, they have an exponentially small bandwidth forming an essentially sharp energy level and are dynamically very distinct from b electrons, being much slower and much more easily localizable. Because of this difference in the nature of the energy distribution of the JT polaronic states, in the lb model for example, the density of polarons decreases only a little with decreasing temperature in the orbital fluid regime in contrast to the expectation in the static polaron model of Millis *et al*. The difference arises from our argument that, even though the adiabaticity parameter $\gamma (=\hbar\omega/t)$ is much less than unity (0.2–0.3) in manganites, one is in the exponentially narrowed polaron bandwidth regime, with the narrowing factor being $\exp(-\lambda/\gamma) \ll 1$. This is in contrast to the well-studied perturbative in γ or Migdal regime [90], where λ needs to be <1, which is not the case for manganites. The general question of the physics of strong electron–phonon coupling is outlined below.

The l polaron–b electron model described above differs from the polaron models used so far for manganites in several significant ways, some already mentioned. First, because of the twofold degeneracy of the e_g level, a two-fluid description is natural. The l polarons, which can form a dense liquid or glass or crystal, are site localized or nearly so. The electrical transport is primarily by the b electrons, though in principle by both l polarons and b electrons. Thus, metallic conduction can coexist with the presence of polarons and will occur when there is a sizeable density of b electrons in the system. In the insulating phase, at high temperatures for instance, when the density of b electrons is low due essentially to the small probability for thermal activation, diffusion (or variable range hopping) of l polarons can contribute significantly to electrical transport. The density and nature (e.g. static/dynamic, size) of the l polaron is expected to change significantly with temperature, doping and chemical identity of the manganite. In this picture, nanoscopic inhomogeneities (of the l and b regions) are inevitable, and are due to Coulomb interactions.

5.2. Electron–phonon coupling

An unresolved question of great basic and current significance insistently thrown up by experimental results on oxides is the physics of large electron–phonon coupling in them, broadly expected because of the relatively localized nature of the unfilled shell d states abetted by electron correlation. Its strength can be characterized by a parameter g in a schematic Holstein-like electron lattice Hamiltonian

$$H_{\text{Holstein}} = -t \sum_{\langle ij \rangle} b_i^+ b_j + g \sum_i n_i x_i + (1/2) \sum_i (K x_i^2 + M^{-1} p_i^2), \tag{11}$$

where x_i is the displacement of a one-dimensional Einstein mode (frequency $\omega_0 = \sqrt{K/M}$) at site i, and n_i is the electron number at site i. The form for a doubly degenerate orbital has been described earlier as H_{JT} (equation (3*a*)). This is also characterized by a single coupling constant g. The dimensionless parameter $\lambda = (g^2/Kt)$ is a measure of its strength *vis-à-vis* the lattice displacement energy $(1/2)Kx_i^2$ and the electron kinetic energy (nearest-neighbour hopping amplitude t, bare bandwidth $2W = 2zt$ for a tight-binding band with z nearest neighbours). Another dimensionless parameter of relevance is the adiabaticity or phonon energy relative to the electron energy, namely $\gamma = (\hbar\omega_0/t)$. For a free electron gas of Fermi energy ε_{F}, the parameter is $(\hbar\omega_0/\varepsilon_{\text{F}})$. In manganites, given the range of values for g, K, t, and ω_0, one has $\lambda \sim 1$–4 and $\gamma \sim 0.2$–0.3. Thus one is in the strong electron–phonon coupling but adiabatic regime.

Figure 8 shows the various regions in the electron–phonon coupling–adiabaticity (λ, γ) plane. The best known is the Migdal [90] or the weak-coupling–adiabatic region, for which one has $\lambda < 1$, and $\gamma \ll 1$, e.g. the free Fermi gas or a Fermi liquid with fast electrons coupled weakly to slow lattice vibrations. Higher-order corrections to the electron–phonon vertex, basically the electron wavefunction modification, are small and weakly perturbative, of relative order $\lambda\gamma$ and higher (since $\lambda < 1$, this translates into $\gamma \ll 1$). It has been realized for a long time [91] and has been recently demonstrated [92, 93] through detailed calculations in the model described by equation (11), that there is an instability for $\lambda = \lambda_{\text{c}} \sim 1$. Migdal theory breaks down. Engelsberg and Schrieffer [94] performed in the 1960s a detailed calculation for a coupled continuum electron–phonon system with free particle dispersion for the unperturbed electrons, an Einstein phonon of bare frequency ω_0 and the electron–phonon coupling equation (11), and concluded that for large λ there is no convergent perturbative expansion. The physical reason is well known:; for large λ, the state with an electron bound by the lattice distortion it causes, namely a small polaron, has lower energy. The zeroth-order electron state wavefunction is not a simple plane wave, and the phonon wavefunction is that of a *displaced* harmonic oscillator. A perturbative description of the lattice undistorted ground state is therefore inappropriate, and such theories are not expected to be convergent. This is most easily reflected in the large electron–phonon-coupling–antiadiabatic or large (λ, γ) region of figure 8. Here the site-localized electron forms a small polaron and the effective intersite hopping is the bare one multiplied by the (initial and final) phonon wavefunction overlap or Franck–Condon factor [68], which is exponentially small: $t_{ij}^* \sim t_{ij} \exp(-\lambda/\gamma) = t_{ij}$. No systematic small perturbative expansion parameter for this regime analogous to $\lambda\alpha$ in the Migdal regime is well known. There can be a small number, namely $\eta = \exp(-\lambda/\gamma)$, but this is not analytic in the possible small parameter (γ).

The manganites (figure 8) are in the regime $\lambda > 1$, $\gamma < 1$, and $(\lambda/\gamma) \gg 1$. In this adiabatic strong-coupling regime it is often assumed quite plausibly that though the ground state is or can be polaronic, the corrections due to the small adiabaticity factor γ are perturbatively small [41, 42]. However, we have taken the view above (sections 2 and 3) that, in this polaronic regime as well, the exponentially small factor $\eta = \exp(-\lambda/\gamma)$ is operative. It reduces the

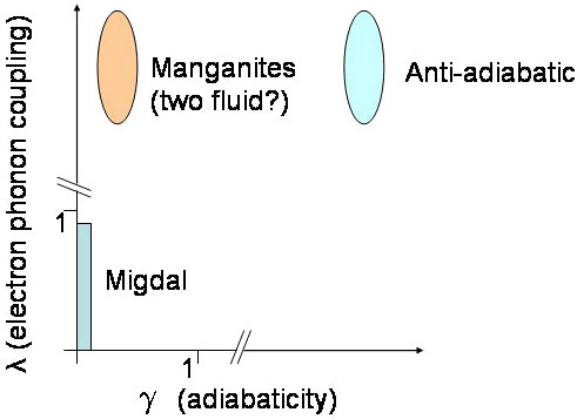

Figure 8. Regions in the electron–phonon-coupling (λ)–adiabaticity (γ) plane. The Migdal, antiadiabatic and manganite regimes are shown.

polaron hopping drastically, and a natural scheme incorporating this effect is the two-fluid (localized-polaron–band-electron) or lb model. The parameter η has an essential singularity at $\gamma = 0$, namely there is no perturbative expansion around the static limit, even for extreme adiabaticity ($\gamma \ll 1$). A simple two-site one-electron model [95, 96] with electron–phonon coupling of the form equation (11) bears this out. In the adiabatic (Born–Oppenheimer) limit $\gamma \to 0$, on solving for the eigenvalues of the Hamiltonian including hopping, one finds that for $\lambda > \lambda_c \sim 1$ there is a twofold degenerate polaronic minimum for the lowest-energy eigenvalue. The kinetic energy term lifts this degeneracy through ion quantum tunnelling. The splitting is exponentially small, approximately $t_{12} \exp(-\lambda/\gamma)$, and is thus perturbatively inaccessible for small γ. A similar result has been obtained for the half-filled Holstein model [97] in the unbroken symmetry phase. Whether this exponentially small polaron energy splitting (appropriately generalized) survives for similar reasons and for arbitrary filling, the effects of orbital degeneracy, of admixture with nonpolaronic broad band states, of a finite density of polarons, of proximity to commensurate densities, of dimensionality and lattice coordination, are questions being explored.

Acknowledgments

I would like to thank the many colleagues and students at the Indian Institute of Science, Bangalore, for introducing me to this fascinating field, for collaboration and for continuing discussions. Some of them are C N R Rao, A K Raychaudhuri, A K Sood, S V Bhat, H R Krishnamurthy, V K Shenoy, G Venketeswara Pai and S R Hassan. I would also like to thank Dr Arindam Chakraborti for crucial help with the manuscript.

References

[1] Kusters R M, Singleton D A, Keen D A, McGreevy R and Hayes W 1989 *Physica* B **155** 362
Chabara K, Ohno T, Kasai M and Kozono Y 1993 *Appl. Phys. Lett.* **63** 1990
von Helmolt R, Wolcker J, Holzapfel B, Schultz M and Samwer K 1993 *Phys. Rev. Lett.* **71** 2331
Jin S, Tiefel T H, McCormack M, Fastnacht R A, Ramesh R and Chen L H 1994 *Science* **264** 413
[2] Jonker G H and van Santen 1950 *Physica* **16** 337
Jonker G H and van Santen 1953 *Physica* **19** 120
[3] Coey J M D, Viret M and von Molnar S 1999 *Adv. Phys.* **48** 167
[4] Salamon M B and Jaime M 2001 *Rev. Mod. Phys.* **73** 583
[5] Dagotto E 2005 *New J. Phys.* **7** 67
[6] Tokura Y 2006 *Rep. Prog. Phys.* **69** 797
[7] Kaplan T A and Mahanti S D (ed) 1999 *Physics of Manganites* (New York: Plenum)
[8] Tokura Y (ed) 2003 *Colossal Magnetoresistive Oxides* (London: Gordon and Breach)

[9] Dagotto E 2002 *Phase Separation and Colossal Magnetoresistance* (Berlin: Springer)
[10] Chatterji T (ed) 2003 *Colossal Magnetoresistive Manganites* (Dordrecht: Kluwer–Academic)
[11] Cheong S-W 2001 private communication
[12] Zhao G, Conder K, Keller H and Muller K A 1996 *Nature* **381** 676
[13] Babushkina N A, Belov L M, Gorbenko O Yu, Kaul A R, Bosak A A, Ozhogin V I and Kugel K I 1998 *Nature* **391** 159
[14] Fäth M, Freisem S, Menovsky A A, Tomioka Y, Aarts J and Mydosh J A 1999 *Science* **218** 805
Renner C, Aeppli G, Kim B G, Soh Y-A and Cheong S-W 2002 *Nature* **416** 518
[15] Uehara M, Mon S, Chen C H and Cheong S-W 1999 *Nature* **399** 560
Sarma D D, Topwal D, Manju U, Krishnakumar S R, Bertolo M, La Rosa S, Cautero G, Koo T Y, Sharma P A and Cheong S-W 2000 *Phys. Rev. Lett.* **93** 09702
[16] Louca D and Egami T 1999 *Phys. Rev.* B **59** 6193
[17] Egami T and Billinge S J L 2002 *Underneath the Bragg Peaks: Structural Analysis of Complex Materials* (Oxford: Pergamon)
[18] Meneghini C, Castellano C, Mobilio S, Kumar A, Ray S and Sarma D D 2002 *J. Phys.: Condens. Matter* **14** 1967
Bindu R, Pandey S K, Kumar A, Khalid S and Pimpale S W 2005 *J. Phys.: Condens. Matter* **17** 6393
[19] Heffner R H, Sonier J E, MacLaughlin D E, Nieuwenhuys G J, Mezei F, Ehlers G, Mitchell J F and Cheong S-W 2003 *Physica* B **326** 494
Allodi G, Cestelli Guidi M, De Renzi R, Caneiro A and Pinsard L 2001 *Phys. Rev. Lett.* **87** 127206
[20] Tranquada J M 2005 *J. Physique* IV **131** 67
Tranquada J M 2005 *Preprint* cond-mat/0508272
[21] Spivak B and Kivelson S A 2004 *Phys. Rev.* B **70** 155114
Jamei R, Spivak B and Kivelson S A 2005 *Phys. Rev. Lett.* **94** 056805
[22] Dagotto E 2005 *Science* **309** 257
[23] Harrison W A 1980 *Electronic Structure and the Properties of Solids* (San Francisco, CA: Freeman)
[24] Sarma D D, Shanthi N, Barman S R, Hamada N, Sawada H and Terakura K 1995 *Phys. Rev. Lett.* **75** 1126
[25] Satpathy S, Popovic Z S and Vukajlovic F R 1995 *Phys. Rev. Lett.* **76** 960
[26] Pickett W E and Singh D J 1996 *Phys. Rev.* B **53** 1146
[27] Popovic Z and Satpathy S 2002 *Phys. Rev. Lett.* **88** 197201
[28] Zenia H, Gehring G A and Timmerman W M 2005 *New J. Phys.* **7** 257
[29] Yin W-G, Volja P and Ku W 2006 *Phys. Rev. Lett.* **96** 116405
[30] Yamasaki A, Feldbacher M, Yang Y-F, Andersen O K and Held K 2006 *Phys. Rev. Lett.* **96** 166401
[31] Millis A J 1997 *Phys. Rev.* B **55** 6405
Feinberg D, Germain P, Grilli P and Siebold G 1998 *Phys. Rev.* B **57** R5583
[32] Zener C 1951 *Phys. Rev.* **82** 403
[33] Anderson P W and Hasegawa H 1955 *Phys. Rev.* **100** 67
[34] Qui X, Proffen Th, Mitchell J F and Billinge S J L 2005 *Phys. Rev. Lett.* **94** 177203
[35] Kanamori J 1960 *J. Appl. Phys.* **31** S14
[36] Millis A J 1996 *Phys. Rev.* B **53** 8434
[37] Iliev M N, Abrashev M V, Popov V N and Hadjiev V G 2003 *Phys. Rev.* B **67** 213201
[38] Millis A J 1998 *Phil. Trans. R. Soc.* A **356** 1473
[39] Ellemaans J B A A, van Laar B, van der Veer K J R and Loopstra B O 1971 *J. Solid State Chem.* **3** 238
[40] Finch G I, Sinha A P B and Sinha K P 1957 *Proc. R. Soc.* A **242** 28
[41] Millis A J, Littlewood P B and Shraiman B I 1995 *Phys. Rev. Lett.* **74** 5144
[42] Millis A J, Shraiman B I and Muller R 1996 *Phys. Rev. Lett.* **77** 175
Millis A J, Muller R and Shraiman B I 1996 *Phys. Rev.* B **54** 5389
Millis A J, Muller R and Shraiman B I 1996 *Phys. Rev.* B **54** 5405
[43] Weisse A and Fehske H 2004 *New J. Phys.* **6** 158
[44] Park J-H, Chen C T, Cheong S-W, Bao W, Meigs G, Chakarian V and Idzerda Yu 1996 *Phys. Rev. Lett.* **76** 4215
[45] Ahn K H and Millis A J 2000 *J. Appl. Phys.* **87** 5013
[46] Ahn K H and Millis A J 2001 *Phys. Rev.* B **64** 115103
Calderon M J, Millis A J and Ahn K H 2003 *Phys. Rev.* B **68** 100401R
[47] Furukawa N and Motome Y 2005 *J. Phys. Soc. Japan* **74** 203
[48] Nakajima T, Yoshizawa H and Ueda Y 2004 *J. Phys. Soc. Japan* **73** 2283
[49] Rodriguez-Martinez L M and Attfield J P 1996 *Phys. Rev.* B **54** 15622
[50] Sawaki Y, Takenaka K, Osuka A, Shizaki R and Sugai S 2000 *Phys. Rev.* B **61** 11588
[51] Zheng G and Patterson C H 2003 *Phys. Rev.* B **67** 220404
Ferrari V, Towler M and Littlewood P B 2003 *Phys. Rev. Lett.* **91** 227202
[52] Loa I, Adler P, Grzechik A, Syassen K, Schwarz U, Hanfland M, Rozenberg Kh G, Goredetsky P and Pasternak M P 2001 *Phys. Rev. Lett.* **87** 125501

[53] Furukawa N 1994 *J. Phys. Soc. Japan* **63** 3214
Furukawa N 1995 *J. Phys. Soc. Japan* **64** 2754
Furukawa N 1999 *Physics of Manganites* ed T A Kaplan and S D Mahanti (New York: Plenum)
[54] Georges A, Kotliar G, Krauth W and Rozenberg M J 1996 *Rev. Mod. Phys.* **68** 13
[55] Li Q, Zang J, Bishop A R and Soukoulis C M 1997 *Phys. Rev.* B **56** 4541
[56] Ramakrishnan T V, Krishnamurthy H R, Hassan S R and Pai G V 2004 *Phys. Rev. Lett.* **92** 157203
[57] Ramakrishnan T V, Krishnamurthy H R, Hassan S R and Pai G V 2003 *Preprint* cond-mat/0308396
[58] Pai G V 2001 *PhD Thesis* Indian Institute of Science, Bangalore, unpublished
[59] Hassan S R 2003 *PhD Thesis* Indian Institute of Science, Bangalore, unpublished
[60] Pai G V, Hassan S R, Krishnamurthy H R and Ramakrishnan T V 2003 *Europhys. Lett.* **64** 696
[61] Edwards D M 2002 *Adv. Phys.* **51** 1259
[62] Roder H, Zang J and Bishop A R 1996 *Phys. Rev. Lett.* **76** 1356
[63] Ishihara S, Inoue J and Maekawa S 1997 *Phys. Rev.* B **55** 8280
Ishihara S, Yamanaka M and Nagaosa N 1997 *Phys. Rev.* B **56** 686
[64] Moreo A, Mayr M, Feiguin A, Yunoki S and Dagotto E 2000 *Phys. Rev. Lett.* **84** 5568
[65] Burgy J, Moreo A and Dagotto E 2004 *Phys. Rev. Lett.* **92** 097202
[66] Kirkpatrick S 1973 *Rev. Mod. Phys.* **43** 574
[67] Murakami S and Nagaosa N 2003 *Phys. Rev. Lett.* **90** 197201
[68] Huang K and Rhys F 1950 *Proc. R. Soc.* A **204** 206
[69] Ramakrishnan T V and Pai G V 2002 *J. Low Temp. Phys.* **126** 1055
[70] Lang I G and Firsov Yu A 1964 *Sov. Phys.—Solid State* **5** 2049
[71] Zang J, Bishop A R and Roder H 1996 *Phys. Rev.* B **53** R8840
[72] Diesenhofer T *et al* 2005 *Phys. Rev. Lett.* **95** 257202
[73] Downward L, Bridges F, Bushart S, Neumeier J J, Dilley N and Zhou L 2005 *Phys. Rev. Lett.* **95** 257202
[74] Kumar P S, Joy P A and Date S K 1998 *J. Phys.: Condens. Matter* **10** L269
Daoud-Alladine A, Rodriguez Carvajal J, Pisard-Gaudart W L, Fernandez-Diaz M L and Revcolevschi A 2002 *Phys. Rev. Lett.* **89** 097205
[75] Freericks J F and Zlatic V 2003 *Rev. Mod. Phys.* **75** 1333
[76] Adams C P, Lynn J W, Smolyaninova V N, Biswas A, Greene R L, Ratcliffe W H, Cheong S-W, Mukovskii Y and Shulyatev D A 2004 *Phys. Rev.* B **70** 134414
[77] Bocquet A E, Mozokawa T, Saitoh T, Namatame H and Fujimori A 1992 *Phys. Rev.* B **46** 3771
[78] Mannella N *et al* 2005 *Nature* **438** 474
[79] Okimoto Y, Katsufuji T, Ishikawa T, Urushibara A, Arima T and Tokura Y 1995 *Phys. Rev. Lett.* **75** 109
Okimoto Y, Katsufuji T, Ishikawa T, Arima T and Tokura Y 1997 *Phys. Rev.* B **55** 4206
[80] Bjornsson P, Rubhausen M, Backstrom J, Kall M, Erikson S, Eriksen J and Borgesson L 2000 *Phys. Rev.* B **61** 1193
[81] Takenaka K, Sawaki Y and Sugai S 1999 *Phys. Rev.* B **60** 13011
Takenaka K, Shiozaku R and Sugai S 2002 *Phys. Rev.* B **65** 184436
[82] Shenoy V B, Gupta T, Krishnamurthy H R and Ramakrishnan T V 2006 *Preprint* cond-mat/0606660
[83] Emery V J and Kivelson S A 1993 *Physica* C **209** 597
[84] Holstein T 1959 *Ann. Phys.* **8** 325
Holstein T 1959 *Ann. Phys.* **8** 343
[85] Narimanov E E and Varma C M 2007 *Preprint* cond-mat/0110047
[86] Argyriou P N, Lynn J W, Osborn R, Campbell B, Mitchell J F, Ruett U, Bordallo H N, Wildes A and Ling C D 2002 *Phys. Rev. Lett.* **89** 036401
[87] Jung J H, Kim K H, Noh T W, Choi E J and Yu J 1998 *Phys. Rev.* B **57** R11043
Kim K H, Jung J H and Noh T W 1998 *Phys. Rev. Lett.* **81** 1517
[88] Chuang Y-D, Gromko A D, Dessau D S, Kimura T and Tokura Y 2001 *Science* **292** 1509
[89] Alexandrov A S and Bratkowsky A M 1999 *J. Phys.: Condens. Matter* **11** 1989
[90] Abrikosov A A, Gorkov L P and Dzhyaloshinskii I E 1963 *Methods of Quantum Field Theory in Statistical Physics* (New York: Dover)
[91] Kohn W and Vachaspati 1951 *Phys. Rev.* **83** 462
[92] Deppeler A and Millis A J 2002 *Phys. Rev.* B **65** 100301
[93] Hague J P and d'Ambrumenil N 2001 *Preprint* cond-mat/0106355
[94] Engelsberg S and Schrieffer J R 1963 *Phys. Rev.* **131** 993
[95] Alexandrov A S 2001 *Europhys. Lett.* **56** 92
[96] Krishnamurthy H R 2005 unpublished
[97] Benedetti P and Zeyher R 1998 *Phys. Rev.* B **58** 14320